

Monte Carlo Simulation of Boltzmann Equation in Space Plasma at High Latitudes

Imad A. Barghouthi*, Naji A. Qatanani[†] and Fathi M. Allan[‡]

Abstract — The Monte Carlo method was shown to be a very powerful technique in solving the Boltzmann equation by particle simulation. Its simple concept, straightforward algorithm, and its adaptability to include new features (such as, gravity, electric field, geomagnetic field, and different collision models) make it useful tool in space plasma physics, and a powerful test of results obtained with other mathematical methods. We have used Monte Carlo method to solve Boltzmann equation, which describes the motion of a minor ion in a background of ions under the effect of external forces and Coulomb collisions with background ions. We have computed the minor ion velocity distribution function, drift velocity, density, temperatures and heat fluxes. As an application, Monte Carlo simulation method has been adapted to determine the O^+ velocity distribution function, O^+ density, O^+ drift velocity, O^+ temperatures, and O^+ heat fluxes for Coulomb Milne problem.

Keywords: Monte Carlo simulation, Boltzmann equation, Milne problem, Coulomb collision, Space Plasma.

Mathematical reviews index: 65C05,76P05

1 Introduction

Computer simulation is an essential tool in studying the space plasma physics. Simulation allows us to develop and test models, to evaluate approximate theories of space plasma, and to obtain detailed information about the ion velocity distribution function and its moments (i.e. density, drift velocity, temperature, heat flux, ...) at different altitudes. The plasma medium, such as the polar wind, ionosphere, magnetosphere, and plasmasphere, consists of ions, electrons and neutral atoms. The motion of these species under the effect of geomagnetic field, gravitational field, polarization electric field and the interactions between them is very difficult to understand. However, Monte Carlo simulation can offer detailed information describing the motion of the plasma constituents and some of the interactions between plasma species. In dealing with plasma it is convenient to describe each species in the plasma by a separate velocity distribution

*Department of Physics, P.O.Box 20002, Al-Quds University, Jerusalem, Palestine

[†]Department of Mathematics, P.O.Box 20002, Al-Quds University, Jerusalem, Palestine

[‡]Department of Mechanical Engineering, MIT, 77 Mass. Ave. Cambridge MA 02139.

function $f_s(\mathbf{v}_s, \mathbf{r}_s, t)$. The velocity distribution function is defined such that $f_s(\mathbf{v}_s, \mathbf{r}_s, t)d\mathbf{v}_s d\mathbf{r}_s$ represents the number of particles of species s which at time t have velocity between \mathbf{v}_s and $\mathbf{v}_s + d\mathbf{v}_s$ and positions between \mathbf{r}_s and $\mathbf{r}_s + d\mathbf{r}_s$. The evolution in time of the species velocity distribution function is determined by the net effect of collisions and the flow in phase space of species under the effect of external forces. The mathematical description of this evolution is given by the well-known Boltzmann equation [17]

$$\frac{\partial f_s}{\partial t} + \mathbf{v}_s \cdot \nabla f_s + \left(\frac{e_s}{m_s}\right) \left[\mathbf{E} + \frac{\mathbf{v}_s \times \mathbf{B}}{c}\right] \cdot \nabla_{v_s} f_s = \frac{\delta f_s}{\delta t} \quad (1)$$

where e_s and m_s are the charge and mass of species s respectively, \mathbf{E} is the electric field, \mathbf{B} is the geomagnetic field, c is the speed of light, ∇ is the coordinate space gradient, and ∇_{v_s} is the velocity space gradient. The quantity $\left(\frac{\delta f_s}{\delta t}\right)$ in the Boltzmann equation represents the rate of change of f_s in a given region of phase space as a result of collisions. For collisions governed by inverse power potentials and for resonant charge exchange collisions, the appropriate expression for $\left(\frac{\delta f_s}{\delta t}\right)$ is the Boltzmann collision integral [17], which is given by

$$\frac{\delta f_s}{\delta t} = \sum_t \int d^3v_t d\Omega g_{st} \sigma_{st}(g_{st}, \theta) [f'_s f'_t - f_s f_t] \quad (2)$$

where d^3v_t is the velocity space volume element of species t , \mathbf{g}_{st} is the relative velocity of the colliding particles s and t , $\sigma_{st}(g_{st}, \theta)$ is the differential scattering cross section, θ is the scattering angle, $d\Omega$ is the element of solid angle in the s particle reference frame, and the primes denote quantities evaluated after collision.

Because the plasma flow conditions can vary markedly within a given region or from one region to another, several different mathematical approaches have been used over the years. These include hydromagnetic, hydrodynamic, generalized transport, kinetic, semi-kinetic, and hybrid particle-in-cell models [9].

In this paper we will solve in details the Boltzmann equation given in (1) by using the Monte Carlo method (i.e. we will find the velocity distribution function f_s , density n_s , drift velocity u_s , parallel $T_{s\parallel}$ and perpendicular $T_{s\perp}$ temperatures, and parallel q_s^{\parallel} and perpendicular q_s^{\perp} heat fluxes). As an example we will use the Monte Carlo method to find the O^+ velocity distribution function and its moments to Coulomb Milne problem.

2 Monte Carlo Method

Monte Carlo method has the advantage that one follows the motion of the individual particles and, hence, a lot of the important physics can be included self-consistently. The standard procedure of the Monte Carlo simulation is to

follow the motion of one ion for a large number of collisions, and to continually monitor its velocity. Then, various kinds of time averages for the ion are computed, which can be equal to the corresponding ensemble averages of the system. In practice, the ion motion is simulated as follows. An ion is injected into the simulation region with an initial velocity that is randomly generated such that it is consistent with the ion velocity distribution function immediately below the simulation region. The time interval between every two successive collisions is found via a proper random number generator. The ion trajectories during these intervals are determined by the classical laws of motion of a charged particle under the influence of gravitational, electric, and geomagnetic fields. Changes of ion's velocity due to collisions are determined using another set of random numbers having the statistical properties determined according to the chosen collision model. Then a suitable grid in velocity space at different altitudes in the simulation region is used to register the ion's behavior. The time that an ion spends in each bin, divided by the bin's volume, is taken to be proportional to the ion's velocity distribution function at its center [6, 7]. Moreover, the individual segments of the trajectory can be directly used to find different velocity moments (i.e. density, drift velocity, temperature, heat flux,...). In the following sections we will explain in details each step of the above Monte Carlo strategy.

3 Generation of ion's velocity

The starting point of most space plasma simulations is the injection of an ion into the simulation region with random initial velocity that corresponds to the ion distribution function at the injection point. In most space plasma applications [3, 4, 12, 14, 16] the initial ion velocity distributions assumed to be non-drifting Maxwellian

$$f(v) = n \left[\frac{m}{2\pi kT} \right]^{\frac{3}{2}} e^{-mv^2/2kT} \quad (3)$$

where, n is the number density, k is the Boltzmann constant, T is the temperature at the injection point (boundary condition), m is the mass of the ion, and \mathbf{v} is the random velocity of the injected ion. In most applications [2, 8, 10], the direction of \mathbf{v} is taken either parallel or perpendicular to the geomagnetic field \mathbf{B} , therefore it is recommended to write v^2 as $v^2 = v_{\parallel}^2 + v_{\perp}^2$ this leads to

$$f(v) = n \left[\frac{m}{2\pi kT} \right]^{\frac{3}{2}} e^{\frac{-m}{2kT}(v_{\parallel}^2 + v_{\perp}^2)} \quad (4)$$

Equation (4) can be written as

$$\begin{aligned}
f(v) &= n \left[\left(\frac{m}{2\pi kT} \right)^{1/2} e^{\frac{-m}{2kT} v_{\parallel}^2} \right] \left[\left(\frac{m}{2\pi kT} \right) e^{\frac{-m}{2kT} v_{\perp}^2} \right] \\
&= n f(v_{\parallel}) f(v_{\perp})
\end{aligned} \tag{5}$$

with

$$f(v_{\parallel}) = \left[\frac{m}{2\pi kT} \right]^{\frac{1}{2}} e^{\frac{-m v_{\parallel}^2}{2kT}}$$

$$f(v_{\perp}) = \left[\frac{m}{2\pi kT} \right] e^{\frac{-m v_{\perp}^2}{2kT}}$$

where $f(v_{\parallel})$ and $f(v_{\perp})$ are the injected ion's velocity distribution function parallel and perpendicular to the geomagnetic field respectively. We will use these distributions to generate the parallel $v_{\parallel s}$ and the perpendicular $v_{\perp s}$ velocities of the injected species.

3.1 Generation of $v_{\perp s}$

We need to get values of the random variable $v_{\perp s}$ (ion's perpendicular velocity) at the injection point which is distributed over the interval $(0, \infty)$ with probability density [1]

$$p(v_{\perp s}) = 2\pi v_{\perp s} f(v_{\perp s})$$

The values of $v_{\perp s}$ are given by

$$\int_0^{v_{\perp s}} P(v'_{\perp s}) dv'_{\perp s} = G, \tag{6}$$

where G is a random number between $(0, 1)$, that is, taking each value of G in turn, we must solve equation (6) and find the corresponding value of $v_{\perp s}$ which is showed to be

$$v_{\perp s}^2 = - \left(\frac{2kT_s}{m_s} \right) \ln(1 - G) \tag{7}$$

In other words, $v_{\perp s}$ is the perpendicular velocity of the randomly injected ion at the bottom boundary.

3.2 Generation of $v_{\parallel s}$

Here, we need to distinguish between the local number of ions with $v_{\parallel s}$ and the actual number of those ions that can cross the lower boundary of the simulation region (i.e. those ions with $v_{\parallel s} < 0$ will not cross the assumed injected boundary).

The probability of finding an ion crossing the lower boundary is proportional to the flux of those ions (i.e. the probability of those ions with $v_{\parallel s} > 0$ which they can reach and cross the lower boundary) and is given by

$$p(v_{\parallel s}) = p(v_{\parallel s})_{local} \times v_{\parallel s} \times \alpha \quad (8)$$

where

$$p(v_{\parallel s})_{local} = f(v_{\parallel s}) = \left[\frac{m_s}{2\pi k T_s} \right]^{\frac{1}{2}} e^{\frac{-m_s}{2k T_s} v_{\parallel s}^2} \quad (9)$$

and α is normalizing constant (i.e. $\int_0^\infty p(v_{\parallel s}) dv_{\parallel s} = 1$).

Hence, we obtain the formula for the probability density

$$p(v_{\parallel s}) = 2\pi v_{\parallel s} \left[\frac{m_s}{2\pi k T_s} \right] e^{\frac{-m_s}{2k T_s} v_{\parallel s}^2} \quad (10)$$

Similarly, we showed the values of the ion's parallel velocity $v_{\parallel s}$ to be given by

$$v_{\parallel s}^2 = - \left(\frac{2k T_s}{m_s} \right) \ln(1 - G). \quad (11)$$

We should note that the formulas for $v_{\parallel s}$ and $v_{\perp s}$ are similar, but they have different numerical values because of G . Now, we randomly generated an ion from Maxwellian distribution at the boundary level.

4 Coulomb Collision

In the collision-dominated plasma, the injected test ion interacts with target of the background ions. Assume the background ions (target) to have a Maxwellian distribution at equilibrium temperature T_t

$$f(v_t) = n_t \left[\frac{m_t}{2\pi k T_t} \right]^{\frac{3}{2}} e^{-m_t v_t^2 / 2k T_t}. \quad (12)$$

Similarly to the previous section, we generate the perpendicular velocity of the target ions by

$$v_{\perp t}^2 = - \left(\frac{2k T_t}{m_t} \right) \ln(1 - G) \quad (13)$$

The generation of $v_{\parallel t}$ is different from the previous section, since we are generating the parallel velocity of an ion from the whole distribution $-\infty < v_{\parallel t} < +\infty$ and not as before from the upper half of the distribution ($v_{\parallel s} > 0$)

$$f(v_{\parallel t}) = n_t \left[\frac{m_t}{2\pi k T_t} \right]^{\frac{1}{2}} e^{-m_t v_{\parallel t}^2 / 2k T_t} = p(v_{\parallel t}) \quad (14)$$

$$G = \int_{-\infty}^{v_{\parallel t}} p(v'_{\parallel t}) dv'_{\parallel t} = \frac{1}{2} \left[1 + \operatorname{erf} \left(\left(\frac{m_t}{2k T_t} \right)^{1/2} v_{\parallel t} \right) \right] \quad (15)$$

$$v_{\parallel t} = \left(\frac{2k T_t}{m_t} \right)^{1/2} \operatorname{erf}^{-1}(2G - 1) \quad (16)$$

Now we will simulate the collision between the test ions and the target ions. The Coulomb force between s ions and t ions is inversely proportional to the square of the interparticle distance. For such a long-range (Coulomb collision) interaction, the collision term given in equation (2) reduces to the well-known Fokker-Planck form [9, 10, 11]

$$\frac{\delta f_s}{\delta t} = -\frac{\partial}{\partial \mathbf{v}_s} \cdot \left[\mathbf{A}_s f_s - \frac{1}{2} \frac{\partial}{\partial \mathbf{v}_s} \cdot \mathbf{D}_s f_s \right] \quad (17)$$

where \mathbf{A}_s is the friction coefficient and \mathbf{D}_s is the diffusion coefficient tensor given by

$$\mathbf{D}_s = D_{s\parallel} \mathbf{e}_z \mathbf{e}_z + D_{s\perp} (\mathbf{I} - \mathbf{e}_z \mathbf{e}_z) .$$

The expressions for $\mathbf{A}_s, D_{s\parallel}$, and $D_{s\perp}$ are given by Hinton [11]

$$\mathbf{A}_s(v) = \frac{-2\Gamma_s n_t z_t^2}{2k T_t / m_t} \left(1 + \frac{m_s}{m_t} \right) G \left(\frac{v}{[2k T_t / m_t]^{1/2}} \right) \quad (18)$$

$$D_{\parallel s}(v) = \frac{2\Gamma_s}{v} n_t z_t^2 G \left(\frac{v}{[(2k T_t) / m_t]^{1/2}} \right) \quad (19)$$

$$D_{\perp s}(v) = \frac{\Gamma_s}{v} n_t z_t^2 \left[\Phi \left(\frac{v}{[(2k T_t) / m_t]^{1/2}} \right) - G \left(\frac{v}{[(2k T_t) / m_t]^{1/2}} \right) \right] \quad (20)$$

$$\Gamma_s = 4\pi z_s^2 e^4 (\ln \Lambda) / m_s^2 \quad (21)$$

where z_t and z_s are the ions charge numbers, n_t is the density of the background (target ions), $\ln \Lambda$ is the Coulomb logarithm, and for most densities and temperatures of interest it is in the range (15 – 20), $\Phi \left(\frac{v}{[(2k T_t) / m_t]^{1/2}} \right)$ is the error function, and

$$G \left(\frac{v}{\sqrt{(2k T_t) / m_t}} \right) = \frac{\Phi \left(\frac{v}{[(2k T_t) / m_t]^{1/2}} \right) - \left(\frac{v}{[(2k T_t) / m_t]^{1/2}} \right) \frac{\partial}{\partial v} \Phi \left(\frac{v}{[(2k T_t) / m_t]^{1/2}} \right)}{2 \left(\frac{v^2}{(2k T_t) / m_t} \right)} \quad (22)$$

is the Chandrasekhar function [11]. It is important to note that Coulomb interaction is analogous to a combination of dynamic friction corresponding to the drag term (\mathbf{A}_s) and diffusion corresponding to the scattering of the test ions in velocity space $D_{\perp s}$ and $D_{\parallel s}$. The test ion is considered to move for a short interval of time Δt . The effect of Coulomb collisions on the velocity of the test ion during the period Δt is implemented at the end of Δt . The period should be chosen small enough so that the test ion velocity \mathbf{v}_s , and, consequently, $\mathbf{A}_s(v_s)$, $D_{\parallel s}(v_s)$ and $D_{\perp s}(v_s)$, can be considered constant during Δt . On the other hand, the computational resources impose limitations on how small Δt can be chosen. We tested the above Fokker-Planck collision model by considering a simple case (homogenous O^+ background with a Maxwellian velocity distribution) for which the exact solution (i.e. f_s) should be Maxwellian with temperature equal to that of the background O^+ . We ran the model for this special case for different values of Δt . The results were compared to the exact solution, and consequently a Δt was chosen that struck a compromise between speed and accuracy. The adopted value for the collision time Δt was chosen to be $0.01v_s/A_s$. The cumulative effect of Coulomb collision during Δt is given by [11, 18]

$$\begin{aligned}\Delta \mathbf{u} &= \mathbf{A}_s \Delta t & (23) \\ \langle (\Delta v_{\parallel s})^2 \rangle &= D_{\parallel s} \Delta t \\ \langle (\Delta v_{\perp s})^2 \rangle &= 2D_{\perp s} \Delta t\end{aligned}$$

where $\Delta \mathbf{u}$ is the change of the test ion velocity due to friction, $\langle (\Delta v_{\parallel s})^2 \rangle$, and $\langle (\Delta v_{\perp s})^2 \rangle$ are the variances of the change in the test ion velocity due to diffusion (in velocity space) in the direction parallel and perpendicular to the original velocity \mathbf{v}_s respectively. We have to decide the sign of $\Delta v_{\parallel s}$ and $\Delta v_{\perp s}$ either positive or negative, because they are randomly distributed, therefore we will generate a random number G between $(0, 1)$ and when G is greater or equal 0.5 we will pick up the positive sign and if G is less than 0.5 we will pick up the negative sign. Now we are able to calculate the test ion velocities $v'_{\parallel s}$, $v'_{\perp s}$ and v'_s after collision

$$\begin{aligned}v'_{\parallel s} &= (v_s + \Delta u + \Delta v_{\parallel s}) \frac{v_{\parallel s}}{v_s} - \left(\frac{\Delta v_{\perp s}}{\sqrt{2}} \right) \frac{v_{\perp s}}{v_s} \\ v'_{\perp s} &= \left[\left[(v_s + \Delta u + \Delta v_{\parallel s}) \frac{v_{\perp s}}{v_s} + \left(\frac{\Delta v_{\perp s}}{\sqrt{2}} \right) \frac{v_{\parallel s}}{v_s} \right]^2 + \frac{(\Delta v_{\perp s})^2}{2} \right]^{1/2} \\ v'_s &= (v'^2_{\parallel s} + v'^2_{\perp s})^{1/2} & (24)\end{aligned}$$

Now we start new step, the new $v'_{\parallel s}$ and $v'_{\perp s}$ for the test ion are respectively given in equations (24).

The new Δt is given by $\left(\frac{0.01v'_s}{A_s(v'_s)}\right)$, the test ion will move during the interval under the effect of external forces (gravity \mathbf{g} , electric field \mathbf{E} and geomagnetic field \mathbf{B}). The change in the test ion velocity due to these forces for the period Δt is calculated from classical laws of physics. The geomagnetic field \mathbf{B} was assumed to be radial. The gravitational potential energy is given by $\Phi_g = -\gamma m_s M_E / r$ where γ is the gravitational constant, M_E is the earth mass, and r is the geocentric distance. The polarization electric field is given by $eE_p = -\partial\Phi_p/\partial r$ where $\Phi_p = kT_e \ln n_e + \text{constant}$, with T_e and n_e are the temperature and density of the electrons respectively. Usually, both electrons and background ions are assumed to be isothermal and have equal temperatures.

The above procedure is repeated until the test ion exists the simulation tube at either top boundary or lower boundary, then another test ion is initiated at the lower boundary. The test ions are monitored as they cross a predetermined set of altitudes.

5 Distribution function

In each simulation (10^5) test ions were monitored as they drifted across the simulation region. At each altitude, a two dimensional grid in velocity space ($v_{\parallel s}, v_{\perp s}$) is used to register their behavior. The time spent by the test ion in each bin of the velocity grid, divided by that bin's volume, was proportional to the test ion velocity distribution at the center of that bin [5]. The symmetry in the azimuthal direction is used to simplify the registration process, therefore, the bin's volume in velocity space is $\Delta^3 v = 2\pi v_{\perp} \Delta v_{\parallel} \Delta v_{\perp}$ and the number of test ions with velocities between \mathbf{v} and $\mathbf{v} + d\mathbf{v}$ is $f_s(v) d^3 v$.

The time that an ion spends in each bin is proportional to the time needed for the test ion to cross the bin; therefore, it equals the width of the bin divided by the parallel velocity $v_{\parallel s}$ (i.e., $t = c_1/|v_{\parallel s}|$) where c_1 is arbitrary constant. The above facts lead to

$$f_s(v) = \frac{c_2}{|v_{\parallel s}|} / (2\pi v_{\perp s} \Delta v_{\parallel s} \Delta v_{\perp s}). \quad (25)$$

Let the width of the bin's sides equals to $\frac{1}{3} \left(\frac{2kT_t}{m_t}\right)^{\frac{1}{2}}$ (i.e., $\frac{1}{3}$ of the thermal speed of the background ions). Therefore, $\Delta v_{\parallel} = \Delta v_{\perp} = \frac{1}{3} \left(\frac{2kT_t}{m_t}\right)^{\frac{1}{2}}$. Note that the volume of the bin does not change, but it differs from the other bin's volume, this makes $f_s(v) = \frac{c}{|v_{\parallel s}|}$ where c is a constant, knowing the parallel ($v_{\parallel s}$) and perpendicular ($v_{\perp s}$) velocities of the test ion at the predetermined altitude help us in locating the test ion in the corresponding bin. The location of the test ion will be determined by two integers (J and I) where $J = INT(3 \times v_{\perp s})$. Note that the distribution is symmetric for v_{\parallel} around v_{\perp} , therefore J takes the

integers from 0 to 10. The maximum value for J was chosen to be 10, because it corresponds to a velocity three times higher than the thermal velocity of the background ions, which is difficult for the test ion to reach. To make sure that we are not sorting outside the array we put a restriction on J such that $J = \text{Min}(J, 10)$. According to the parallel direction, the boundaries of the bins are set at $(-9.5, -8.5, \dots, 8.5, 9.5)$ where the integer I taken to be $I = \text{NINT}(3 \times v_{\parallel s})$ between $(-10, 10)$. Each bin will be known by $(J, I, \text{altitude})$. After we have determined the location of the test ion (i.e., the bin) we put the numerical value of $f_s(v_s)$ in that bin, and when another test ion crosses that altitude and located into that bin we add the numerical value of $f_s(v_s)$ to the previous one. We kept doing the above test for all test ions.

6 Moments of the distribution function

In this section we will determine the moments of the distribution function (i. e. density, drift velocity, parallel and perpendicular temperatures, and parallel and perpendicular heat fluxes). The test ion distribution function can be represented as

$$f_s(v_s) = 9c_2 \sum_i \frac{1}{|v_{\parallel s}^i|} \frac{\delta(v_{\parallel s} - v_{\parallel s}^i) \delta(v_{\perp s} - v_{\perp s}^i)}{2\pi v_{\perp s}^i} \quad (26)$$

where $\delta(x)$ is the Dirac delta function [5], the superscript i is used to denote that the summation is over all continuous segments of the test ion trajectory in velocity space. With this expression, it is possible to accumulate the data necessary to compute the above velocity moments while following the test ion's motion. In the following sub-sections we obtained the definitions for the velocity moments from [19].

6.1 Density

$$\begin{aligned} n_s &= \int f_s(v_s) d^3v_s = 2\pi \int f_s(v_s) dv_{\parallel s} v_{\perp s} dv_{\perp s} \\ &= 9c_2 \sum_i 2\pi \int \frac{\delta(v_{\perp s} - v_{\perp s}^i) \delta(v_{\parallel s} - v_{\parallel s}^i) dv_{\parallel s} v_{\perp s} dv_{\perp s}}{2\pi |v_{\parallel s}^i| v_{\perp s}^i} \\ &= 9c_2 \sum_i \frac{1}{|v_{\parallel s}^i|} . \end{aligned} \quad (27)$$

Therefore, after the specification of the location of the test ion (i.e., the bin) we add to the density store $\frac{1}{|v_{\parallel s}^i|}$.

6.2 Drift velocity

The drift velocity u of the test ions s is equal to the expectation value of $v_{\parallel s}$ (i.e., $\langle v_{\parallel s} \rangle$)

$$\begin{aligned}
 u_s &= \frac{\int v_{\parallel s} f_s(v_s) d^3 v_s}{\int f_s(v_s) d^3 v_s} \\
 u_s &= \frac{\int dv_{\parallel s} v_{\perp s} dv_{\perp s} 2\pi \sum_i \frac{\delta(v_{\perp s} - v_{\perp s}^i) \delta(v_{\parallel s} - v_{\parallel s}^i)}{2\pi |v_{\parallel s}^i| v_{\perp s}^i} v_{\parallel s}}{\int dv_{\parallel s} v_{\perp s} dv_{\perp s} 2\pi \sum_i \frac{\delta(v_{\perp s} - v_{\perp s}^i) \delta(v_{\parallel s} - v_{\parallel s}^i)}{2\pi |v_{\parallel s}^i| v_{\perp s}^i}} \\
 &= \sum_i \frac{v_{\parallel s}^i}{|v_{\parallel s}^i|} / \sum_i \frac{1}{|v_{\parallel s}^i|} = \frac{\sum_i \text{sign}(v_{\parallel s}^i)}{\sum_i \frac{1}{|v_{\parallel s}^i|}}.
 \end{aligned} \tag{28}$$

6.3 Perpendicular temperature

The random thermal velocity is defined as $\mathbf{c}_s = \mathbf{v}_s - \mathbf{u}_s$. The thermal energy $\frac{3}{2}kT_s$ is the expectation value for the kinetic energy ($\frac{1}{2}m_s c_s^2$) i.e.,

$$\frac{3}{2}kT_s = \frac{\int \frac{1}{2}m_s [(v_{\parallel s} - u_s)^2 + v_{\perp s}^2] f_s(v_s) d^3 v_s}{\int f_s(v_s) d^3 v_s} \tag{29}$$

$$\frac{1}{2}kT_{\parallel s} + kT_{\perp s} = \frac{\int \frac{1}{2}m_s (v_{\parallel s} - u_s)^2 f_s(v_s) d^3 v_s}{\int f_s(v_s) d^3 v_s} + \frac{\int \frac{1}{2}m_s v_{\perp s}^2 f_s(v_s) d^3 v_s}{\int f_s(v_s) d^3 v_s}. \tag{30}$$

From equation (30) the perpendicular temperature is given by the expectation value of $T_{\perp s} = \frac{1}{k} \langle (\frac{1}{2}m_s v_{\perp s}^2) \rangle$, i. e. the second term of equation (30).

$$T_{\perp s} = \frac{m_s}{2k} \frac{\sum_i (v_{\perp s}^i)^2 / |v_{\parallel s}^i|}{\sum_i \frac{1}{|v_{\parallel s}^i|}}. \tag{31}$$

6.4 Parallel temperature

According to equation (30) the parallel temperature is defined as

$$\begin{aligned}
 T_{\parallel s} &= \frac{m_s}{k} \frac{\int (v_{\parallel s} - u_s)^2 f_s(v_s) d^3 v_s}{\int f_s(v_s) d^3 v_s} \\
 T_{\parallel s} &= \frac{m_s}{k} \left[\int v_{\parallel s}^2 f_s(v_s) d^3 v_s - 2u_s \int v_{\parallel s} f_s(v_s) d^3 v_s + u_s^2 \right] / \int f_s(v_s) d^3 v_s
 \end{aligned}$$

$$T_{\parallel s} = \frac{m_s}{k} \left[\frac{\sum_i (v_{\parallel s}^i)^2 / |v_{\parallel s}^i|}{\sum_i \frac{1}{|v_{\parallel s}^i|}} - \left(\frac{\sum_i \text{sign}(v_{\parallel s}^i)}{\sum_i \frac{1}{|v_{\parallel s}^i|}} \right)^2 \right]. \quad (32)$$

6.5 Parallel heat flux

$$\begin{aligned} q_s^{\parallel} &= \frac{1}{n_s} \left(\frac{m_s}{2kT_s} \right)^{\frac{3}{2}} \int d^3 v_s (v_{\parallel s} - u_s)^3 f_s(v_s) \\ &= \frac{1}{n_s} \left(\frac{m_s}{2kT_s} \right)^{\frac{3}{2}} \left[v_{\parallel s}^3 f_s(v_s) d^3 v_s - 3u_s \int v_{\parallel s}^2 f_s(v_s) d^3 v_s \right. \\ &\quad \left. + 3u_s^2 \int v_{\parallel s} f_s(v_s) d^3 v_s - u_s^3 \int f_s(v_s) d^3 v_s \right] \\ &= \left(\frac{m_s}{2kT_s} \right)^{\frac{3}{2}} \left[\frac{\sum_i (v_{\parallel s}^i)^3 / |v_{\parallel s}^i|}{\sum_i \frac{1}{|v_{\parallel s}^i|}} - \frac{3u_s \sum_i (v_{\parallel s}^i)^2 / |v_{\parallel s}^i|}{\sum_i \frac{1}{|v_{\parallel s}^i|}} \right. \\ &\quad \left. + \frac{3u_s^2 \sum_i v_{\parallel s}^i / |v_{\parallel s}^i|}{\sum_i \frac{1}{|v_{\parallel s}^i|}} - \frac{u_s^3 \sum_i 1 / |v_{\parallel s}^i|}{\sum_i \frac{1}{|v_{\parallel s}^i|}} \right]. \end{aligned} \quad (33)$$

6.6 Perpendicular heat flux

$$\begin{aligned} q_s^{\perp} &= \frac{1}{2n_s} \left(\frac{m_s}{2kT_s} \right)^{\frac{3}{2}} \int d^3 v_s (v_{\parallel s} - u_s) v_{\perp s}^2 f_s(v_s) \\ &= \left(\frac{m_s}{2kT_s} \right)^{\frac{3}{2}} \left[\frac{1}{2} \frac{\sum_i v_{\parallel s}^i v_{\perp s}^i / |v_{\parallel s}^i|}{\sum_i \frac{1}{|v_{\parallel s}^i|}} - \frac{\frac{1}{2} u_s \sum_i (v_{\perp s}^i)^2 / |v_{\parallel s}^i|}{\sum_i \frac{1}{|v_{\parallel s}^i|}} \right]. \end{aligned}$$

In the previous sections we found the solution of the Boltzmann equation, *i.e.* $f_s(v_s)$ and the velocity moments of the distribution function.

7 Application: Coulomb Milne Problem

In this section we apply the previous solution of the Boltzmann equation for the outflow of ions in an ions background (*i.e.*, $s = O^+$ and $t = H^+$), this problem is similar to Milne problem [13, 15]. We assume Maxwellian distribution for H^+ ion in the simulation region extended from (200 km to 5500 km), the O^+ distribution at the boundary is non-drifting Maxwellian. The test O^+ ion is considered to move for a short period of time Δt under the effect of Coulomb collisions. A

large number of O^+ ions (10^5) were followed (one at a time) as they moved until existed the simulation region. The O^+ velocity distribution function as well as the altitude profiles of its moments (density, drift velocity, parallel and perpendicular temperature, parallel and perpendicular heat flux), and the results are presented in Fig.(1) and Fig.(2) respectively. For simplicity, we presented the results of the Coulomb Milne problem in terms of a normalizing quantities,

$$\begin{aligned}\tilde{v}_{O^+} &= v_{O^+} / \left(\frac{2kT_{H^+}}{m_{O^+}} \right)^{1/2}; & \tilde{u}_{O^+} &= u_{O^+} / \left(\frac{2kT_{H^+}}{m_{O^+}} \right)^{1/2}; \\ \tilde{T}_{\parallel O^+} &= T_{\parallel O^+} / T_{H^+}; & \tilde{T}_{\perp O^+} &= T_{\perp O^+} / T_{H^+}; \\ \tilde{q}_{O^+}^{\parallel} &= q_{O^+}^{\parallel} / \left[m_{O^+} n_{O^+} \left(\frac{2kT_{H^+}}{m_{O^+}} \right)^{3/2} \right]; \\ \tilde{q}_{O^+}^{\perp} &= q_{O^+}^{\perp} / \left[m_{O^+} n_{O^+} \left(\frac{2kT_{H^+}}{m_{O^+}} \right)^{3/2} \right].\end{aligned}\quad (34)$$

Figure 1 shows the O^+ velocity distribution function $f(O^+)$ at three altitudes (200 km, 1000 km, and 5000 km) that correspond to different collision conditions. In the collision dominated region (bottom panel), the $f(O^+)$ is very close to Maxwellian, which is consistent with the assumed condition at the injection point. As altitudes increases the O^+ distribution in the transition region becomes drifting Maxwellian (middle panel) and close to bi-Maxwellian at 5000 km in the collisionless region (top panel). Figure 2 shows the moment profiles for O^+ ions. The top left panel shows the O^+ density profile, the density decreases, with altitude, which means that the majority of O^+ ions are in the collision-dominated region at low altitude coupled with the background H^+ ions via Coulomb collision. The top right panel shows the O^+ drift velocity, it increases with altitudes, because the O^+ ions are coupled with the H^+ ions in the collision dominated region, but those fast O^+ ions are less coupled and they can escape to a higher altitude collisionless region where collisions are less effective. The profiles for O^+ parallel and perpendicular temperatures are given in the bottom left panel. At low altitude both temperatures are equal to the temperature of the background due to O^+ coupling with H^+ via Coulomb collision. At high altitude and for large velocities, the velocity diffusion in the perpendicular direction dominates ($D_{O^+ \perp} \approx \frac{1}{v_{O^+}} \gg D_{O^+ \parallel} \approx \frac{1}{v_{O^+}^3}$), this gives more heating to the perpendicular direction than parallel direction, this explain the increasing in perpendicular temperature compared to parallel temperature, and explains the bi-Maxwellian features of $f(O^+)$ at higher altitude. The bottom right panel of Fig. 2 shows the profile of heat fluxes for the parallel and perpendicular energies, at low altitude, both heat fluxes are positive and increase with altitude.

At middle altitudes both heat fluxes components are positive and rapidly $\tilde{q}_{O^+}^\perp$ changes from positive maximum to minimum and then starts to increase in the collisionless region, however, $\tilde{q}_{O^+}^\parallel$ changes from positive maximum at 1800 km to negative minimum at 4500 km and then starts to increase.

8 Conclusion

The present work has showed the usefulness and importance of Monte Carlo method in the solution of the Boltzmann equation. It is anticipated that this method of solution will prove more efficient than kinetic and transport approaches, particularly in applications to realistic system (solar wind, polar wind, ionosphere, ...) and in following the motion of plasma constituents under the effect of external forces (gravity, electric field, geomagnetic field) and interactions (Polarization, Resonance charge exchange, Coulomb) between plasma species. A Monte Carlo solution to the Boltzmann equation has been presented. The major steps of the Monte Carlo simulation are:

1. Test ion (minor) is randomly generated (i.e $v_{\parallel s}$ and $v_{\perp s}$ are determined) from a non-drifting Maxwellian distribution with temperature T_s at the bottom boundary.
2. The time interval Δt between Coulomb collisions is randomly generated via a proper random number generator.
3. The final velocity of the minor ion due to the external forces (gravitational, electric, and geomagnetic) is computed during the above time interval Δt .
4. A major ion from the background is randomly generated (i.e $v_{\parallel t}$ and $v_{\perp t}$ are determined) from a Maxwellian distribution of temperature T_t .
5. The effect of Coulomb collisions during the time interval Δt is implemented at the end of Δt and the changes in the minor ion's velocity are determined.
6. The above steps (motion under the effect of external forces followed by Coulomb collisions) are repeated until the minor ion exits from the simulation region at the top or the bottom boundaries: then another minor ion is injected at the lower boundary.

7. The minor ions are monitored as they cross a predetermined set of altitudes, and the minor ion velocities are used to accumulate the information needed to compute the source velocity distribution function f_s and the moments of the distribution function (density, drift velocity, temperatures and heat fluxes).

As an application, O^+ outflow in H^+ background has been described. The quantities $f(O^+)$, \tilde{u}_{O^+} , $\tilde{T}_{O^+\parallel}$, $\tilde{T}_{O^+\perp}$, $\tilde{q}_{O^+\parallel}$, and $\tilde{q}_{O^+\perp}$ have been computed, and these new results are part of an on going extended study.

We believe that the Monte Carlo simulation of Boltzmann equation in space plasma at high latitude presented here provide the best description to date of the ion velocity distribution and its moments in the presence of gravitational field, polarization electric field, geomagnetic field and Coulomb collisions, primarily because of the self-consistent handling of the Coulomb collisions.

References

- [1] C. Aldrich, Particle code simulations with injected particles, *Space science reviews*, 42, 131 (1985).
- [2] A. Barakat, and I. Barghouthi, The effect of wave-particle interaction on the polar wind O^+ , *Geophys. Res. Lett.* 21, 2279 (1994).
- [3] A. Barakat, and I. Barghouthi, The effect of wave-particle interaction on the polar wind: Preliminary results, *Planet. and Space Sci.*, 42, 987 (1994).
- [4] A. Barakat, and J. Lemaire, Monte Carlo study of the escape of a minor species, *Phys. Rev. A*, 42, 3291 (1990).
- [5] A. Barakat and R. Schunk, Comparison of Maxwellian and bi-Maxwellian expansions with Monte Carlo simulations for anisotropic plasmas, *J. Phys. D*, 15, 2189 (1982).
- [6] I. Barghouthi, Effects of wave-particle interactions on H^+ and O^+ outflow at high latitude: A comparative study, *J. Geophys. Res.*, 102, 22, 065 (1997).
- [7] I. Barghouthi, A. Barakat, and A. Persoon, The effects of altitude-dependent wave-particle interactions on the polar wind plasma, *Astrophysics and space sciences*, 259, 117 (1998).
- [8] I. Barghouthi and A. Barakat, Comparison between the wave-particle interaction in the polar wind and in the auroral region, *physics of space plasma*, 13, 445 (1995).

- [9] I. Barghouthi, A. Barakat, and R. Schunk, Monte Carlo study of the transition region in the polar wind: An improved collision model, *J. Geophys. Res.* 98, 17, 583 (1993).
- [10] I. Barghouthi, V. Pierrad, A. Barakat, and J. Lemaire, A Monte Carlo simulation of the polar wind: Effect of velocity distributions with kappa suprathermal tails, *Astrophysics and space Sciences*, 277, 427 (2001).
- [11] F. Hinton, Collision transport in plasma, in *basic plasma physics 1*, edited by A. Galeev and R. Sudan (North-Holland, New York, 1983), p. 147.
- [12] J. Lemaire, and M. Scherer, kinetic models of the solar and polar winds, *Rev. Geophys.*, 11, 427 (1973).
- [13] ϕ . Lie-Svendensen and M Rees, An improved kinetic model for the polar wind outflow of a minor ion, *J. Geophys. Res.*, 101, 2415 (1996).
- [14] J Lemaire and V. Pierrad, polar and solar winds, *Astrophysics and space sciences*, 277, 169 (2001).
- [15] M. Lindenfeld and B. Shizgal, The Milne problem: A study of the mass dependence, *Phys. Rev. A*, 27, 1657 (1983).
- [16] V. Pierrard and J. Lemaire, Lorentzian ion exosphere model, *J. Geophys. Res.*, 101, 7923 (1996).
- [17] R. Schunk, Mathematical structure of transport equations for multispecies flows, *Rev. Geophys.*, 15, 429 (1977).
- [18] L. Spitzer and M. Hart, Random gravitational encounters and the evolution of spherical systems, 1, *Method, Astrophys. J.*, 164, 399 (1971).
- [19] C. Zamlutti, Transport equations for multicomponent isotropic and anisotropic high speed space plasmas, *planet. Space Sci.*, 42, 557 (1994).

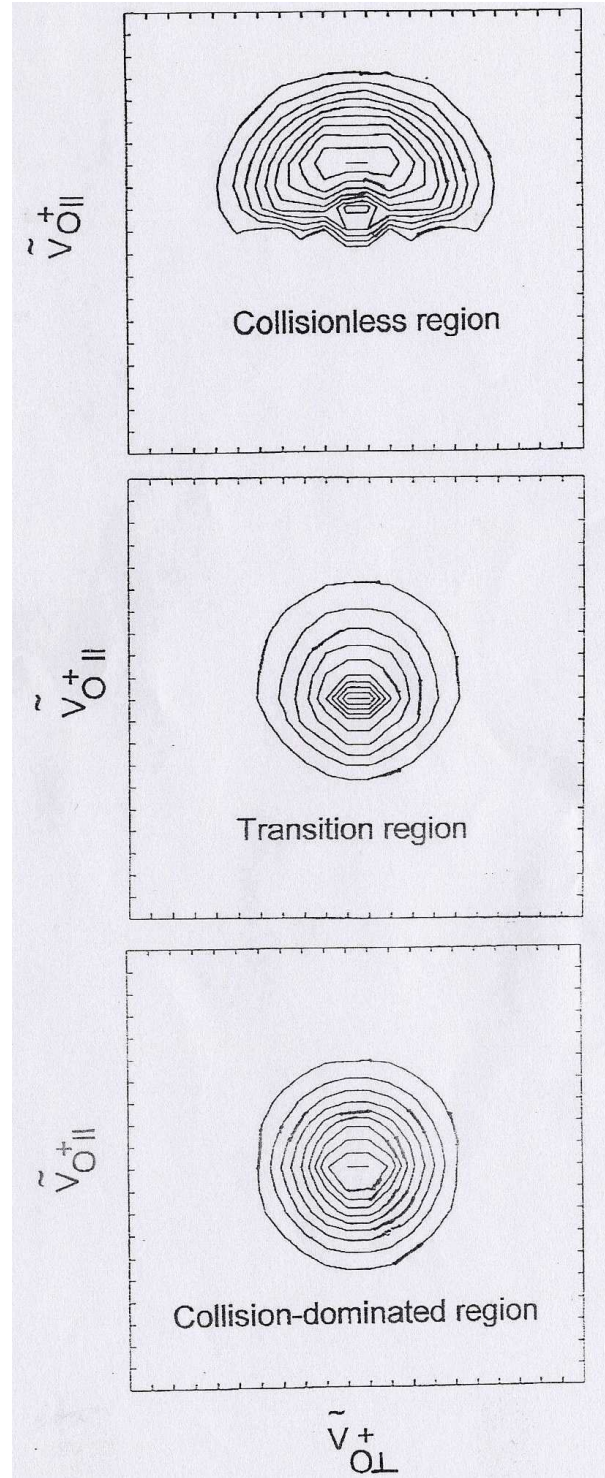


Figure 1: The O^+ velocity distribution function for Coulomb Milne problem, f_{O^+} is represented by equal value contours in the velocity plane $(\tilde{v}_{O\perp}^+, \tilde{v}_{O\parallel}^+)$, where $\tilde{v}_{O^+} = v_{O^+}/(2kT_{H^+}/m_{O^+})^{1/2}$. The contour levels decrease successively by a factor of $e^{1/2}$ from the maximum, which is marked by a dot. The center of each plot corresponds to zero velocity. The axes are calibrated in multiples of $\frac{1}{3}(2kT_{H^+}/m_{O^+})^{1/2}$.

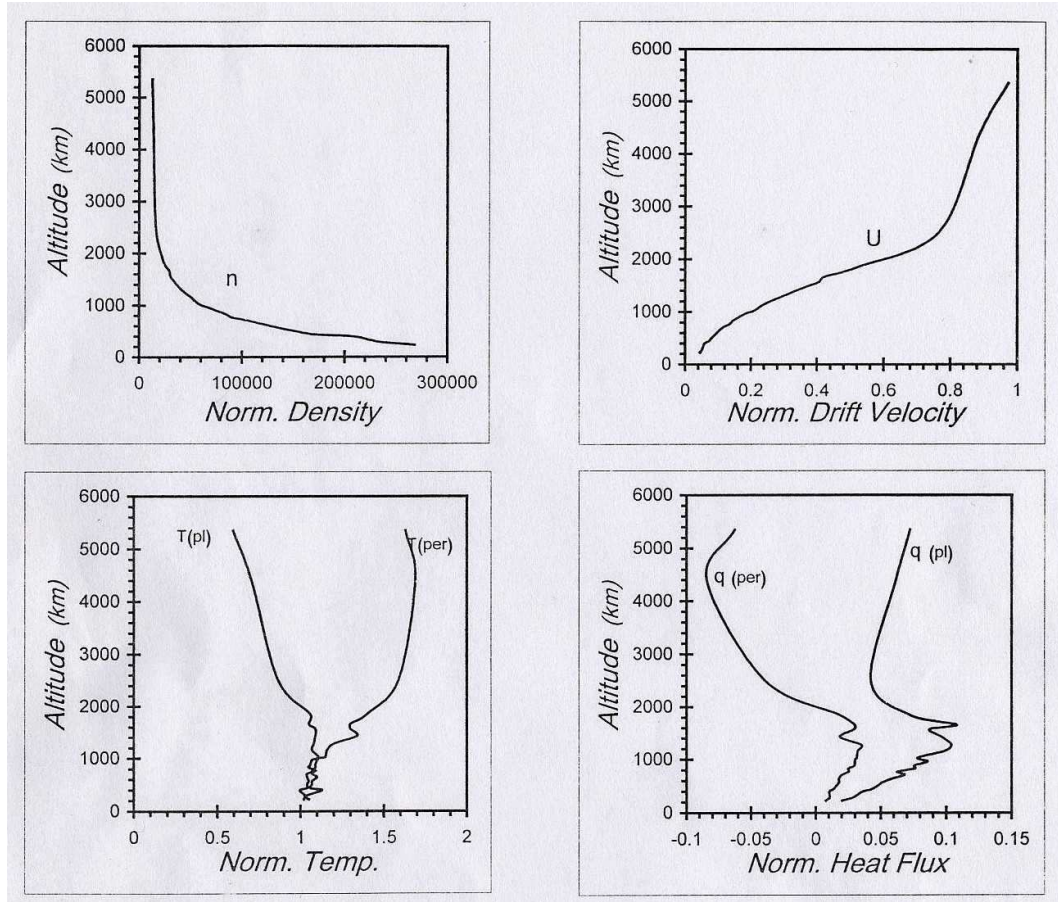


Figure 2: Altitude profiles of the different O^+ moments for Coulomb Milne problem. The normalized moments considered here are (top left) density \tilde{n}_{O^+} , (top right) drift velocity \tilde{u}_{O^+} (bottom left), parallel $\tilde{T}_{\parallel O^+}$, and perpendicular $\tilde{T}_{\perp O^+}$ temperatures, and (bottom left) the parallel $\tilde{q}_{\parallel O^+}$ and perpendicular $\tilde{q}_{\perp O^+}$ fluxes.